Hyperfine Interactions 123/124 (1999) 667–680

Transverse coherence in nuclear resonant scattering of synchrotron radiation

Alfred Q.R. Baron

SPring-8, 323-3 Mihara, Mikazuki-cho, Sayo-gun, Hyogo 679-5198, Japan
E-mail: baron@spring8.or.jp

We discuss the effects of transverse coherence in time domain nuclear resonant scattering experiments using synchrotron radiation. The importance of source and detector sizes, as well as the Fresnel zone size of the sample are described. These effects are demonstrated in experiments using a rotating stainless-steel foil [1]. The emphasis of the text is to provide simple physical explanations while mathematical details are discussed in the appendix.

1. Introduction

The purpose of this article is to provide an introduction to transverse coherence and its effects in nuclear resonant scattering (NRS) experiments.[1] In the context of NRS measurements it is usually the longitudinal coherence, being directly related to the long nuclear lifetime, that attracts interest. However, precisely because many synchrotron based experiments are scattering measurements using a very small source (the electron beam in the storage ring), one must consider the effects of transverse correlations in the scattered wave field, and how they relate to both the sample being investigated and the experimental setup. This can provide additional information about a sample and also adds some subtlety to the interpretation of NRS experiments.

The background for this work is recent interest in transverse coherence in X-ray scattering, largely due to the availability of relatively brilliant synchrotron radiation sources (see section II-1 of this issue) as coherence effects typically scale with source brilliance. However, the field of optical coherence (of which X-ray coherence can be considered a very small part) reaches back to the previous century, including both sophisticated formalism and a wide range of experiments [2,3]. Relevant areas of recent interest include X-ray speckle measurements [4,5] and phase-contrast imaging [6,7]. There are also a variety of techniques for directly investigating transverse X-ray coherence [8–13].

In the context of optical coherence, it is worth pointing out that X-ray measurements are very much in their infancy and X-ray sources are still relatively weak. Therefore, here we focus only on the simplest field–field correlations and do not dis-

[1] We refer the reader to the other sections of this issue for background information on this subject and references.

cuss higher order correlations (e.g., Hanbury-Brown–Twiss intensity correlations [14]) as their effects should, in general, be negligible. We deliberately avoid introducing the extensive formalism from other [2,3] treatments of coherence and focus on physical arguments, with a minimum of mathematics, though some of the details of the calculations may be found in the appendix.

2. Transverse coherence length

The relevant figure of merit for many X-ray measurements is the transverse coherence length, ξ_t. It is essentially the answer to the question: over what length scale, transverse to the beam propagation direction, is there a correlation in the phase and amplitude of a wave field. The simplest examples from optics, monochromatic[2] point sources or plane waves, have essentially infinite transverse coherence lengths, since once the phase and amplitude are defined at one point in space, one knows them for all other points. With synchrotron radiation, one has an effective point source for each photon (the emitting electron or positron in the storage ring) but different photons will come from different electrons (or positrons) in the source and these radiate independently. Practically, experiments are done integrating over many detected photons, so the source size limits the transverse coherence length.

One can get a quantitative estimate for the transverse coherence length in different ways. Very directly, one can ask, given a collection of (independently phased) point sources of some finite size (e.g., the electron beam in the storage ring), and an object plane some distance away, how far can one separate two points in the object plane before the phase difference between them becomes uncertain due to the source size. However, it is more satisfying physically, and practically equivalent, to consider the Fraunhofer diffraction from a double slit (or pinhole) [15]. Then one can ask what is the maximum separation of the two slits (pinholes) placed in the object plane that yields a Fraunhofer diffraction pattern with good visibility. Consider figure 1. The radiation from a single electron located, say, at one edge of the electron beam, may, at the location of the slits, be considered approximately a plane wave. This results in a diffraction pattern with a period of λ/d in the far field. Radiation from another electron on the other side of the source will also generate a diffraction pattern, but it will be displaced in angle from the first, corresponding to the displacement of the electron in the source. Observation of the interference pattern in the far field requires that the angular size of the source, as seen by the slits, is less than the period of the interference pattern. Alternatively, for a fixed source size, one can ask what is the maximum separation of the slits that provides good visibility of the interference pattern. Thus

[2] For nuclear scattering measurements, the bandwidth of the resonance (even when broadened or hyperfine split) is small enough that it is a monochromatic source as regards transverse coherence measurements. More exactly, one requires that all optical path length differences are less than the longitudinal coherence length of the radiation. Typical longitudinal coherence lengths are meters while path length differences are usually μm.

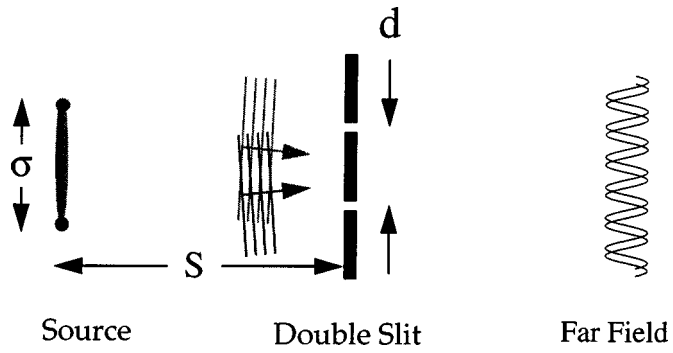

Figure 1. Blurring of a Fraunhofer two slit diffraction pattern due to finite source size.

(considering one dimension only, for the moment) one takes the transverse coherence length at distance S from a source of size σ_0 as

$$\xi_t \approx \frac{\lambda S}{2\pi\sigma_0}. \tag{2.1}$$

Depending on the author, definitions will vary by factors of 2 or π. Explicit calculation for a Gaussian source gives that the Fraunhofer interference pattern for the two slits has the form $I(\Theta) \propto 1 + \mu\cos(2\pi\Theta d/\lambda)$, where Θ is the angle between the center of the slits and the detector point. The amplitude of the interference term is given by $\mu = \exp[-\frac{1}{2}(d/\xi_t)^2]$. If we take the slit separation to be $d = \xi_t$, one has $\mu = 0.6$, while for $d = 3\xi_t$, $\mu \sim 0.01$. Thus, with the definition eq. (2.1) slits separated by ξ_t give relatively good contrast, while the contrast from slits separated by $3\xi_t$ or more can largely be ignored. Typical source sizes at third generation synchrotron radiation facilities are 30–100 μm full width at half maximum (FWHM) vertically ($\sigma_0 = 13$–43 μm) and about an order of magnitude larger horizontally, while source–sample distances are about 50 meters. This gives nominal coherence lengths of about 20–60 μm in the vertical, and 2–5 μm in the horizontal direction.

3. Time domain effects of transverse coherence

The "two slit" discussion can be extended to the time domain by replacing the two slits with two nuclear scatterers. One then asks what time response will be measured by a point-like detector due to the emission of a short pulse of radiation from an electron in the source. Considering only a 2-dimensional case for simplicity, figure 2 shows the relevant quantities. The source–sample and sample–detector distances are S and D, respectively, and the exact locations of the source and detector are displaced a distance y_0 and y_d from the optical axis. The impulse excitation from the source will reach the two scatterers at slightly different times, corresponding to the difference in path lengths from the source. The scatterers then radiate and the relative phasing of the fields at the detector will be further modified by the different path lengths to the detector. This can all be included using appropriate retarded times (see appendix). Taking, for simplicity,

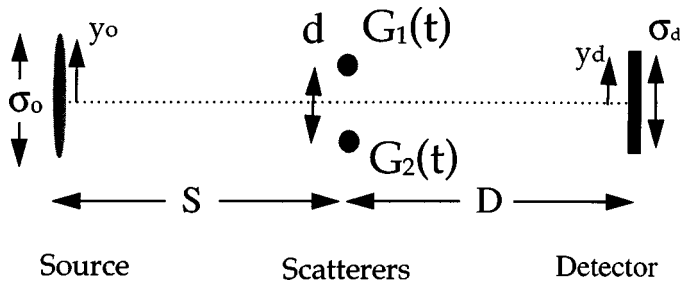

Figure 2. The nuclear scattering (time domain) analogue of the two slit experiment.

the two scatterers to be identical up to a shift in their response frequencies (e.g., an isomer or Doppler induced shift between the two) we have $G_j(t) = G_0(t)\mathrm{e}^{-\mathrm{i}\omega_j t}$ ($j = 1, 2$). The time dependent intensity measured by a point detector at y_d, due to impulse excitation from a point source at y_0, is then

$$I(t) \propto \left|G_0(t)\right|^2 \left[1 + \cos\left\{\Omega t + 2\pi \frac{d}{\lambda}\left(\frac{y_0}{S} + \frac{y_\mathrm{d}}{D}\right)\right\}\right], \tag{3.1}$$

where $\Omega = \omega_2 - \omega_1$. In the simplest case (a thin scatterer or a single nucleus), $G_0(t)$ is an exponential decay and, more generally, might include some Bessel function dependence (for a thick sample, see section IV-2.1 of this issue) and/or hyperfine structure. In any case, the interference (cosine) term shows the expected quantum beat pattern at the difference frequency, Ω, but with a phase determined by the geometry. In an experiment with finite source and detector sizes, this geometry dependent term leads to blurring. In particular, if we take a Gaussian source (σ_0) located at $y_0 = 0$ and a Gaussian detector (σ_d) located at $y_\mathrm{d} = y_D$ (for convenience in getting an analytical form) integration of eq. (3.1) gives

$$I(t) \propto |G_0(t)|^2 \left[1 + \mathrm{e}^{-(1/2)(d/\xi_\mathrm{te})^2} \cos\left\{\Omega t + 2\pi \frac{d}{\lambda}\frac{y_D}{D}\right\}\right], \tag{3.2}$$

where

$$\xi_\mathrm{te} = \frac{\lambda}{2\pi}\frac{1}{\sigma_\Theta}, \quad {\sigma_\Theta}^2 = \left(\frac{\sigma_0}{S}\right)^2 + \left(\frac{\sigma_\mathrm{d}}{D}\right)^2. \tag{3.3}$$

Here one sees that the finite detector size degrades the contrast in a manner completely analogous to that of the finite source size. Thus we extend the definition of the transverse coherence length, ξ_t, to include the effect of finite detector size as well as finite source size, defining an effective transverse coherence length, ξ_te.

4. Experimental results

Demonstration of the effects of transverse coherence requires manipulating the nuclear response on a fairly small length scale and, practically, a “two scatterer”

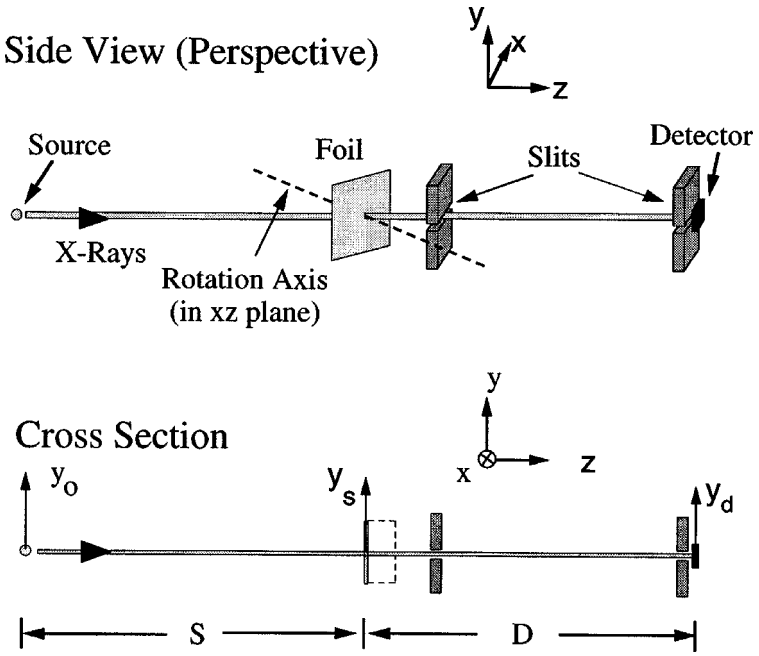

Figure 3. Experimental set-up for the rotating foil experiment.

sample is somewhat difficult to realize. However, demonstration of the main points of the above discussion was possible using a rotating stainless steel (SS) foil. This was discussed in some detail in [1]. Here we show some additional data, highlighting the effects of finite detector and sample sizes, as this is particularly pertinent to our discussion.

The essential idea for the experiment was to create a sample with a continuous change (Doppler shift) in the nuclear response transverse to the beam direction. Rotation of a foil, as shown in figure 3, does precisely this, introducing a convenient one-dimensional gradient in the Doppler shift in the nuclear response frequency. The coherent addition of the scattering from nuclei with a distribution of Doppler shifts, essentially a broadening of the frequency response, is expected to result in a faster decay of the impulse response. More exactly, if the rotation introduces a distribution of frequencies across the foil given by $\Delta\Omega$, then the coherent response of this distribution should decay with a time scale $T_{\rm coh} = 1/\Delta\Omega$. In contrast, incoherent addition of the response of different parts of the foil should lead to the same response as that for the foil at rest. Thus, a faster decay becomes the mark of coherence, much like the contrast of the beats was the indication of coherence in the previous (two scatterer) example.

The expected faster decay was demonstrated in [1], and showed excellent agreement with optical calculations (see the appendix and [1]), as is shown in figure 4. The left hand panel shows the raw data, with the faster decay easily seen as the rotation rate

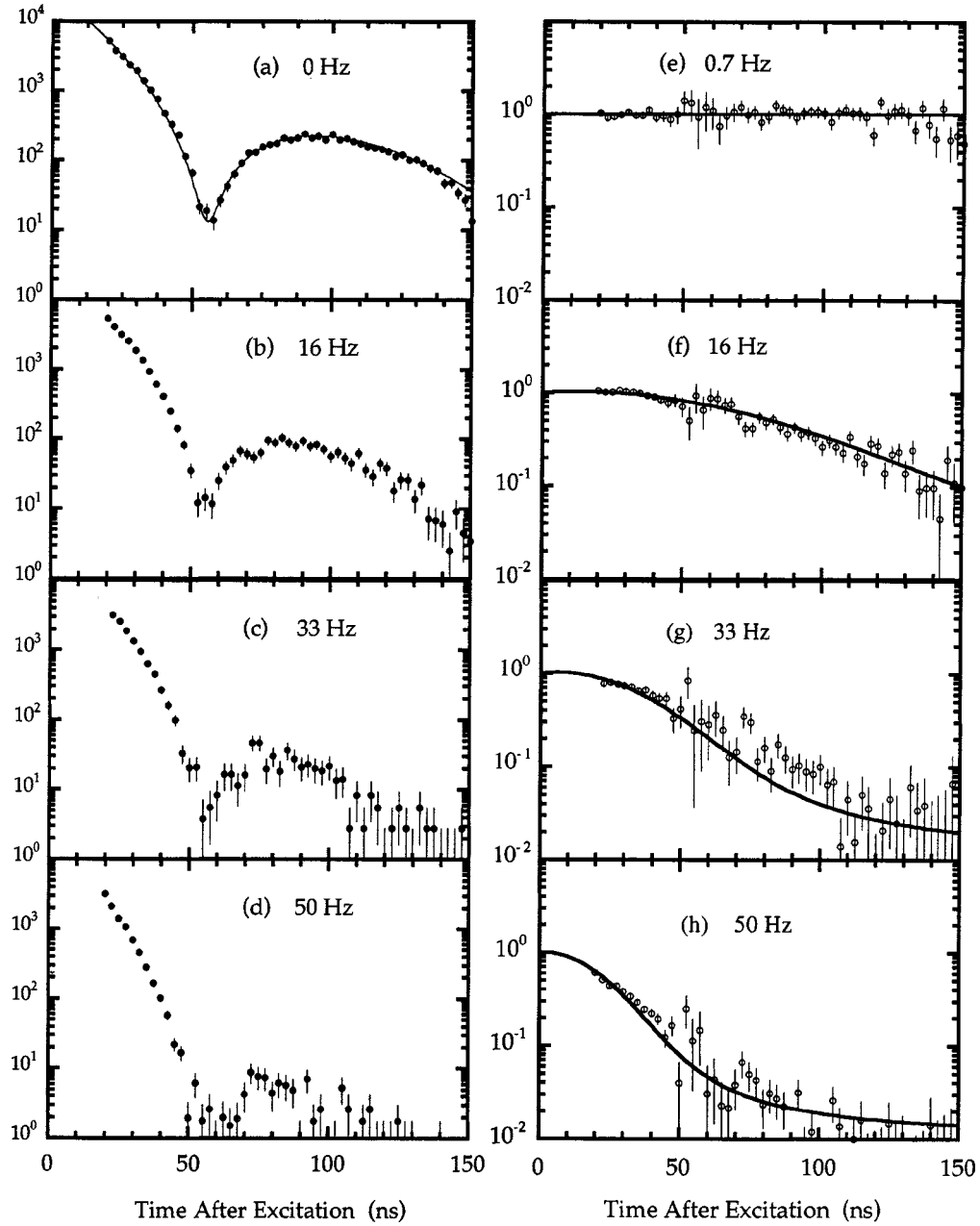

Figure 4. Effect of increasing the rotation rate of the foil on the measured time response (detector and sample sizes both measured to be 15 μm). (a)–(d) show the raw data while (e)–(h) show the data divided by the fit to the response at rest (solid line in (a)) and the calculation (solid lines).

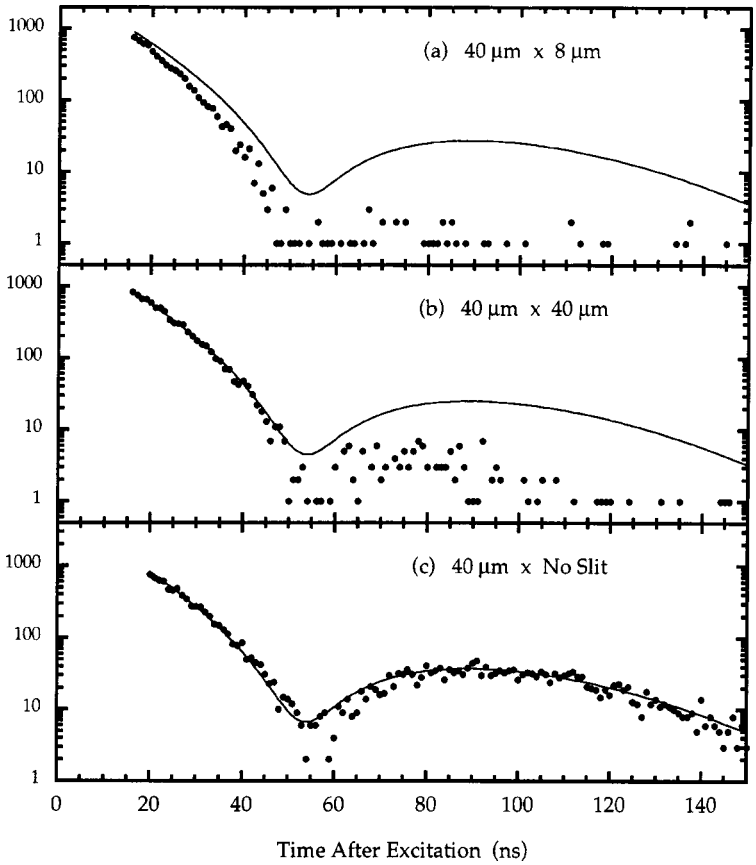

Figure 5. Effect of changing the detector size on the time response. The numbers are the nominal sizes of the slits limiting the sample and the detector, respectively. The solid line is the fit to the response at rest, included as a reference in each figure. Note that slit sizes are calculated based on the thickness of shim material used and are not measured values. It is expected that, particularly at the small (8 μm) size, the actual acceptance was somewhat smaller. Data from [16].

increases, while the right hand panel shows the data divided by the fit to the response at rest, and the calculation.[3]

An analytic solution for the rotating foil is possible if we take Gaussian distributions for the source, sample and detector. We write the solution as [1]

$$\frac{I_{\text{rotating}}(t)}{I_{\text{atrest}}(t)} = \exp\left\{-\frac{1}{2}\left(\frac{t}{T_{\text{coh}}}\frac{\xi}{\sigma_{\text{s}}}\right)^2\right\}. \tag{4.1}$$

[3] The only free parameter in the calculation is the source size, which was determined to be a factor of 5 larger than expected. This was confirmed by another technique [13], and found to be due to the high resolution monochromator (HRM). Subsequent work (K. Fezzaa, A. Baron et al., unpublished) suggests that the presence of a deposit or oxide, as was clearly visible on the surface of the first crystal of the HRM, might account for the degradation of the coherence.

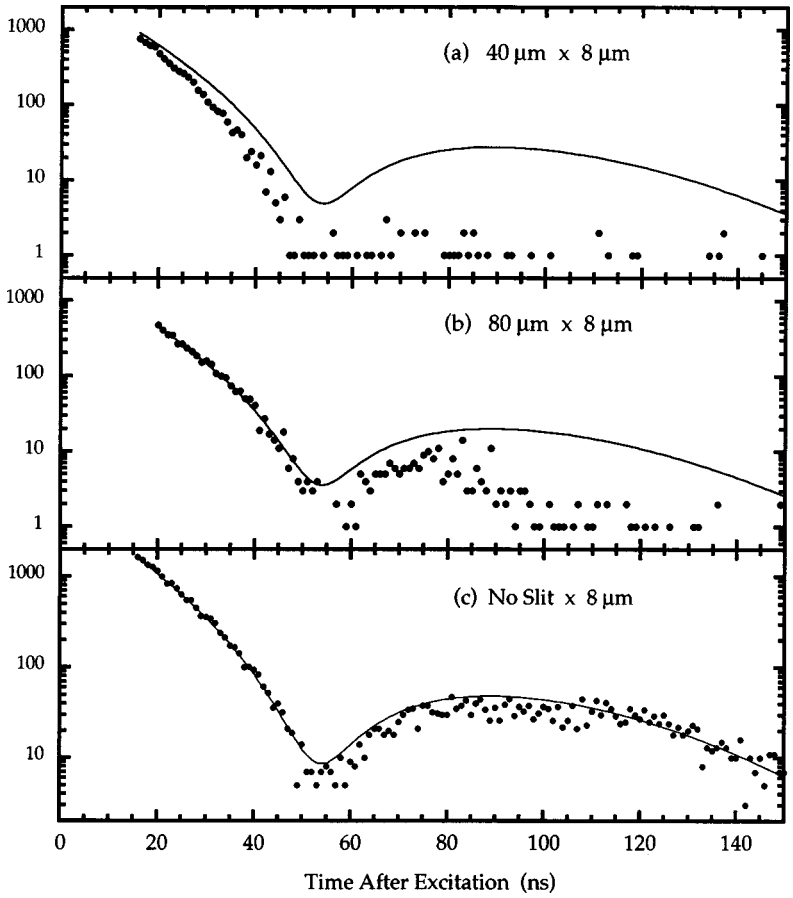

Figure 6. Effect of changing the sample size on the time response. The numbers are the nominal sizes of the slits limiting the sample and the detector, respectively. The solid line is the fit to the response at rest, included as a reference in each figure. See the note about slit sizes in the caption of figure 5. Data from [16].

Here $T_{\rm coh}$ is the decay time expected if the response of the entire sample combined coherently,[4] $\sigma_{\rm s}$ is the sample size and ξ is that part of the sample that acts coherently in the experiment (e.g., leads to a faster response). In particular, one finds

$$\xi = \frac{\lambda}{2\pi\alpha}, \qquad \alpha^2 = \frac{\sigma_0^2}{S^2} + \frac{\sigma_{\rm d}^2}{D^2} + \left(\frac{\sigma_{\rm s}}{D} + \frac{\sigma_{\rm s}}{S}\right)^2 + \frac{1}{\sigma_{\rm s}^2}, \tag{4.2}$$

where σ_0 and $\sigma_{\rm d}$ are the sizes of the source and detector. Then, momentarily neglecting the last two terms in α, one finds that the dependence on source and detector sizes is

[4] The bandwidth due to the Doppler shift from the rotation over a region of the foil of size $\sigma_{\rm s}$ is $\Delta\Omega = k\sigma_{\rm s}\Omega_{SS}$, where Ω_{SS} is the angular velocity of the foil, appropriately projected into the beam direction: i.e., $\Omega_{SS} = 2\pi N \sin\Theta$, where Θ is the angle between the rotation axis and the beam direction ($\pi/4$ in the experiment) and N is the rotation rate of the foil.

identical to that given above (eq. (3.3)): the relevant length scale is exactly the effective transverse coherence length, ξ_{te}. The importance of this term is demonstrated in figure 5, where one sees that the response slows to an incoherent (foil at rest) response as the detector size increases (i.e., the effective transverse coherence length decreases).

The third term in eq. (4.2) is new and deserves comment. Physically, its importance is demonstrated in figure 6, where the measured response is seen to slow down (become incoherent) when the sample is increased in size. Mathematically, it results from including Fresnel (nonlinear) terms in the phase that are important because we are not in a true far-field (Fraunhofer) limit (see appendix). In fact, considering the case where this term dominates the response one finds the relevant length scale in eq. (4.1) is ξ_F/σ_s, where

$$\xi_F = \sqrt{\frac{\lambda}{2\pi}\frac{1}{1/D + 1/S}} \approx \sqrt{\frac{\lambda D}{2\pi}}, \tag{4.3}$$

which is just the size of the first Fresnel zone of the sample (up to the factor 2π – see, e.g., [2, p. 371]). Thus, the interpretation of the third term in α of eq. (4.2) is that sections outside the first Fresnel zone of the sample contribute incoherently to the measured response. The final term in eq. (4.2) just ensures the proper limit in the case of extremely small samples.

5. Application to NRS measurements

In the context of other nuclear scattering experiments, transverse coherence is most relevant to samples where there may be some sort of domain structure, possibly resulting from different chemical or magnetic environments, or from some sort of phase transition. The above discussion shows there are two transverse length scales that are important for determining the coherence of the measured response. The effective transverse coherence length, ξ_{te}, given by eq. (3.3), is sample-independent. Sections of the sample that are separated by more than this amount (say $3\xi_{te}$ or more to reduce effects below the 1% level) will not interfere in a time domain measurement. In a typical experiment, the detector size ($\sigma_d \sim 1$ mm at $D \sim 1$ m) dominates and one has $\xi_{te} \sim 200\lambda$, so sections of the sample separated transversely by distances of order 0.06 μm or more will generally not produce measurable interference. Thus, if a typical experiment shows the presence of interference from different domains, this means that either they are stacked in the direction of beam propagation or they have a rather small length scale.

The Fresnel zone size of the sample, ξ_F, given by eq. (4.3), is also important and sections of the sample that are separated by more than this amount will tend to add incoherently in the detector. However, if this is the limiting term (i.e., if $\xi_{te} > \xi_F \sim 4$ μm for $D = 1$ m, $\lambda = 0.86$ Å) one should really take it as an indication that a detailed model of the sample is necessary. The particular example of a rotating foil showed a general trend toward incoherent response if the sample size exceeded the

Fresnel zone size. However, more generally the response will depend on the details of the domain structure that exists in the sample and the detector position relative to those domains.

Summarizing the above results, the most general rule is that transversely separated sections of a sample will combine incoherently unless their size is both less than the effective transverse coherence length eq. (4.2), and less than the Fresnel zone size eq. (4.3). However, given that these length scales are generally relatively small, the first consideration should be whether or not the sample will have domains stacked along the direction of propagation, as this will always lead to coherent combination of the responses. If, during an experiment, there is some question about the effects of transverse coherence on the time response, a good first test may be to move the detector from, say, $D = 10$ cm to $D = 1$ m. If the measured time response is not affected, then probably transverse coherence, can be ignored at least as far as it might influence a spectroscopic measurement.

One may consider using these effects to investigate correlations in the nuclear response of a sample perpendicular to the beam direction. One may increase the effective transverse coherence length (and Fresnel zone size) to some few microns, allowing investigation of similar sample length scales. However, here one notes there are two complications: on the one hand there is the practical point that this requires a detector that is smaller than the beam size and thereby reduces the intensity in what is already not a high count rate experiment (though this difficulty might be alleviated by using an array detector). On the other hand, while rough length scale information might be obtained by simply correlating changes in the measured time response with the effective transverse coherence length, detailed information and fitting of the time response requires a similarly detailed model of the sample response, which may be somewhat complicated.

Appendix

This appendix presents some of the details of the calculations. The purpose of the presentation is, on the one hand, to facilitate the modification of such calculations by others and, on the other, to clearly indicate what assumptions have been made, and some of the effects of such assumptions. We also point out the general importance of the *effective* transverse coherence length.

Figure 7 indicates the relevant quantities. The source–sample and sample–detector distances are S and D, respectively. The exact locations of the point source, nucleus in the sample and detector point are displaced from their nominal locations by small distances given by $\boldsymbol{\eta}_0$, $\boldsymbol{\eta}_\mathrm{s}$ and $\boldsymbol{\eta}_\mathrm{d}$, respectively. We now take the response of the sample to impulse excitation at $t = t_x$ to be $G(t - t_x, \boldsymbol{\eta}_\mathrm{s})$, where the dependence on $\boldsymbol{\eta}_\mathrm{s}$ is explicitly included to the possibility of the sample response being non-uniform. Then we write the total field, as seen by a particular point in the detector, as the integral

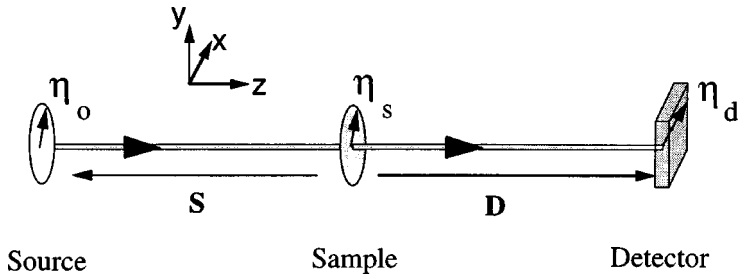

Figure 7. Definition of symbols used in the appendix.

over the sample:

$$E(t, \boldsymbol{\eta}_0, \boldsymbol{\eta}_\mathrm{d}) = \int_{\mathrm{Sample}} G(t - t_{\mathrm{R1}} - t_{\mathrm{R2}}, \boldsymbol{\eta}_\mathrm{s})\, \mathrm{d}\boldsymbol{\eta}_\mathrm{s}, \tag{A.1}$$

where t_{R1} and t_{R2} are the travel times from the source point to the sample point and from the sample point to the detector, respectively.

In the context of nuclear scattering, one must examine G carefully. If we take G as proportional to the (Fourier transform of the) nuclear scattering amplitude, then this equation is a kinematic or Born approximation to the scattering. This would be appropriate in the thin sample limit, where the effect of the downstream part of the sample on the scattering from the upstream part may be ignored. However, practically, almost all samples in nuclear scattering experiments are thick. Thus, the approximation was made to compress the sample into a 2-dimensional one, and take G to be the forward scattering response, including the Bessel function for multiple scattering. In general, for cases where the spread of the wave field inside the sample is not large, this is probably a good approximation. In the experiment described in [1] and the above work, the fact that the location of the minimum of the Bessel function does not shift suggests that this is a reasonable assumption.

We now factor out the nuclear resonance frequency, taking $G(t, \boldsymbol{\eta}_\mathrm{s}) = \mathrm{e}^{-\mathrm{i}\omega_0 t} G_0(t, \boldsymbol{\eta}_\mathrm{s})$ and shift the time by $t_0 = (S + D)/c$, so that $t = 0$ is redefined as the time at which the wave first reaches the detector. One now has

$$E(t, \boldsymbol{\eta}_0, \boldsymbol{\eta}_\mathrm{d}) = \int_{\mathrm{Sample}} G_0(t, \boldsymbol{\eta}_\mathrm{s}) \mathrm{e}^{-\mathrm{i}\omega_0(t + t_0 - t_{\mathrm{R1}} - t_{\mathrm{R2}})}\, \mathrm{d}\boldsymbol{\eta}_\mathrm{s}. \tag{A.2}$$

We have assumed that the dependence on time in G_0 is slow, relative to the path length differences from different parts of the sample, so $t_0 - t_{\mathrm{R1}} - t_{\mathrm{R2}} \approx 0$ in the argument of G_0. The relative phasing is given by

$$\boldsymbol{\Phi} = \omega_0(t_{\mathrm{R1}} + t_{\mathrm{R2}} - t_0) = \frac{\omega_0}{c}\left[|\mathbf{S} + \boldsymbol{\eta}_0 - \boldsymbol{\eta}_\mathrm{s}| + |\mathbf{D} + \boldsymbol{\eta}_\mathrm{d} - \boldsymbol{\eta}_\mathrm{s}| - t_0\right]. \tag{A.3}$$

The general form of these terms is ($k \equiv \omega_0/c = 2\pi/\lambda$)

$$k|\mathbf{S}+\boldsymbol{\eta}| = k\left[S^2+\eta^2+2\mathbf{S}\cdot\boldsymbol{\eta}\right]^{1/2}, \quad |\mathbf{S}| \gg |\eta|$$
$$\approx kS\left[1+\frac{1}{S}\widehat{\mathbf{S}}\cdot\boldsymbol{\eta}+\frac{1}{2S^2}\left(\eta^2-\left(\widehat{\mathbf{S}}\cdot\boldsymbol{\eta}\right)^2\right)\right]. \tag{A.4}$$

Consideration of the magnitude of these terms, $\lambda \sim 10^{-10}$ m, $S > 1$ m, η (sample and source size) $\lesssim 10^{-3}$ m) shows that, in general, the terms of higher than third order can certainly be neglected. Terms of third order might be included, but are generally not interesting because they vary on an essentially macroscopic (mm length) scale. Terms of second order should generally be included for careful calculations, while the first order (Fraunhofer) term dominates. Then, taking a 2-dimensional source and detector, oriented normal to the beam direction ($\mathbf{S}\cdot\boldsymbol{\eta}_0, \mathbf{D}\cdot\boldsymbol{\eta}_\mathrm{d} = 0$), one has

$$\Phi \approx -\mathbf{q}\cdot\boldsymbol{\eta}_\mathrm{s} + k\frac{(\boldsymbol{\eta}_0-\boldsymbol{\eta}_\mathrm{s})^2}{2S} + k\frac{(\boldsymbol{\eta}_\mathrm{d}-\boldsymbol{\eta}_\mathrm{s})^2}{2D} - k\frac{(\widehat{\mathbf{S}}\cdot\boldsymbol{\eta}_\mathrm{s})^2}{2S} - k\frac{(\widehat{\mathbf{D}}\cdot\boldsymbol{\eta}_\mathrm{s})^2}{2D}, \tag{A.5}$$

where $\mathbf{q} = k(\mathbf{D}+\mathbf{S})$ is the usual momentum transfer. Noting that terms independent of η_s can be taken out of the integral and drop out when one squares to get the intensity, we can take

$$\Phi \approx -\boldsymbol{\eta}_\mathrm{s}\cdot\left(\frac{\boldsymbol{\eta}_0}{S}+\frac{\boldsymbol{\eta}_\mathrm{d}}{D}\right)+\eta_\mathrm{s}^2\left(\frac{1}{2S}+\frac{1}{2D}\right). \tag{A.6}$$

We have also taken $\mathbf{q} = 0$ and $\mathbf{S}\cdot\boldsymbol{\eta}_\mathrm{s} \approx 0$ and $\mathbf{D}\cdot\boldsymbol{\eta}_\mathrm{s} \approx 0$, assuming near forward scattering and a thin (2-dimensional) sample (see the discussion above).

At this point we have provided sufficient background to derive all the equations in the text: one may calculate the field by integrating over the scattering from the sample, and then one squares to get the intensity, and then integrate the intensity over the source and detector distributions. For Gaussians, the appropriate integral may be found in [17, p. 485, eq. (3.923)].

We now show the importance of the effective transverse coherence length discussed in the text both explicitly and generally. What we do here really amounts to a special case of a more general formulation of scattering (see, e.g., [2,3]), but we do not introduce an extended notation and explicitly highlight the importance of the effective transverse coherence length. In particular, to see the effect of the finite source and detector size, it is convenient to explicitly introduce them, and calculate the time response one should have in a real experiment. One has[5]

$$I(t) = \int_{\mathrm{Source}} \mathrm{d}\boldsymbol{\eta}_0 W_0(\boldsymbol{\eta}_0) \int_{\mathrm{Detector}} \mathrm{d}\boldsymbol{\eta}_\mathrm{d} W_\mathrm{d}(\boldsymbol{\eta}_\mathrm{d}) \left|E(t,\boldsymbol{\eta}_0,\boldsymbol{\eta}_\mathrm{d})\right|^2, \tag{A.7}$$

where W_0 describes the distribution of electrons in the source and W_d the detector acceptance. Taking these as Gaussians (and assuming they are uncorrelated in the x

[5] If the sample response is not static in time (e.g., due to diffusional motion) one should include a configurational average over sample states as well as the average over the source and detector.

and y directions), and noting that the field depends on the source and detector positions only through the phase, one can perform the integrations to find directly

$$I(t) \propto \int_{\text{Sample}} \mathrm{d}\boldsymbol{\eta}_{\mathrm{s}1}\,\mathrm{d}\boldsymbol{\eta}_{\mathrm{s}2} G_0(t,\boldsymbol{\eta}_{\mathrm{s}1}) G_0^*(t,\boldsymbol{\eta}_{\mathrm{s}2}) \mathrm{e}^{-\mathrm{i}\Phi} \times \mathrm{e}^{-(\eta_{\mathrm{s}1x}-\eta_{\mathrm{s}2x})^2/(2\xi_{\mathrm{te}x}^2)} \mathrm{e}^{-(\eta_{\mathrm{s}1y}-\eta_{\mathrm{s}2y})^2/(2\xi_{\mathrm{te}y}^2)}. \tag{A.8}$$

The double integration over the sample is from the square in eq. (A.7) while the phase is directly obtainable from eq. (A.6).[6] The important point as regards the previous discussion is the presence of the Gaussians from the source and detector integrations. These explicitly limit how far apart two different parts of the sample can be to contribute coherently to the scattering. The length scale is precisely the effective transverse coherence length introduced in the text (only now, since we consider a 2-dimensional sample, the x and y components contribute individually). In particular, we have

$$\xi_{\mathrm{te}y} = \frac{\lambda}{2\pi}\frac{1}{\sigma_{\Theta y}}, \qquad \sigma_{\Theta y}^2 = \left(\frac{\sigma_{0y}}{S}\right)^2 + \left(\frac{\sigma_{\mathrm{d}y}}{D}\right)^2, \tag{A.9}$$

where σ_{0y} is the vertical size of the source and $\sigma_{\mathrm{d}y}$ the vertical size of the detector. A similar expression holds for the horizontal dimensions ($y \to x$).

The above discussion shows, in some generality, how the size of the source and the detector limit the coherent addition of the scattering from transversely separated portions of the sample. In particular, the relevant length scale is precisely the effective transverse coherence length (eqs. (3.3) or (A.9)).

Acknowledgements

The author is grateful to the Nuclear Resonance Group at ESRF (A.I. Chumakov, H.F. Grünsteudel, H. Grünsteudel and R. Rüffer) and L. Niesen (Univ. Groningen) for collaboration on the experimental work discussed here [1,16].

References

[1] A.Q.R. Baron, A.I. Chumakov, H.F. Grünsteudel, H. Grünsteudel, L. Niesen and R. Rüffer, Phys. Rev. Lett. 77 (1996) 4808.
[2] M. Born and E. Wolf, *Principles of Optics* (Pergamon Press, New York, 1980).
[3] L. Mandel and E. Wolf, *Optical Coherence and Quantum Optics* (Cambridge Univ. Press, New York, 1995).
[4] M. Sutton, S.G.J. Mochrie, T. Greytak, S.E. Nagler, L.E. Berman, G.A. Held and G.B. Stephenson, Nature 352 (1991) 608.
[5] S. Brauer, G.B. Stephenson, M. Sutton, R. Brning, E. Dufresne, S.G.J. Mochrie, G. Grübel, J. Als-Nielsen and D.L. Abernathy, Phys. Rev. Lett. 74 (1995) 2010.

[6] One has $\Phi = -k(\boldsymbol{\eta}_{\mathrm{s}1}-\boldsymbol{\eta}_{\mathrm{s}2})\cdot\boldsymbol{\eta}_{\mathrm{d}} + k(\eta_{\mathrm{s}1}^2-\eta_{\mathrm{s}2}^2)(1/(2S)+1/(2D))$, where $\boldsymbol{\eta}_{\mathrm{d}}$ is the location of the center of the detector and the source has been assumed to be located at $\eta_{\mathrm{s}}=0$.

[6] A. Snigirev, I. Snigireva, V. Kohn, S. Kuznetsov and I. Schelokov, Rev. Sci. Inst. 66 (1995) 5486.
[7] P. Cloetens, R. Barrett, J. Baruchel, J. Guigay and M. Schlenker, J. Phys. D: Appl. Phys. 29 (1996) 133.
[8] T. Ishikawa, Acta Crystallogr. A 44 (1988) 496.
[9] T. Salditt, H. Rahn, T.H. Metzger, J. Peisl, R. Schuster and J.P. Kotthaus, Z. Physik B: Condens. Matter 96 (1994) 227.
[10] P. Cloetens, J.P. Guigay, C. De Martino, J. Baruchel and M. Schlenker, Opt. Lett. 22 (1997) 1059.
[11] K. Fezzaa, F. Comin, S. Marchesini, R. Coïsson and M. Belakhovsky, J. X-Ray Sci. Technol. 7 (1997) 12.
[12] D.L. Abernathy, S. Brauer, G. Grübel, I. McNulty, S.G.J. Mochrie, N. Mulders, A.R. Sabdy, G.B. Stephenson and M. Sutton, J. Synchrotron Radiation 5 (1998) 37.
[13] A. Snigirev et al., in preparation.
[14] R. Hanbury-Brown and R.Q. Twiss, Nature 177 (1956) 27.
[15] L. Mandel and E. Wolf, Rev. Mod. Phys. 37 (1965) 231.
[16] A.Q.R. Baron, A.I. Chumakov, H.F. Grünsteudel, H. Grünsteudel, L. Niesen and R. Rüffer, unpublished.
[17] I.S. Gradshteyn and I.M. Ryzhik, *Table of Integrals, Series and Products* (Academic Press, New York, 1980).